Protoplasma (2003) 222: 183–191
DOI 10.1007/s00709-003-0007-5

PROTOPLASMA
Printed in Austria

Actins from plant and animal sources tend not to form heteropolymers in vitro and function differently in plant cells

Y. Jing[1], **K. Yi**[1], and **H. Ren**[1,2,*]

[1] Institute of Cell Biology, Beijing Normal University, Beijing
[2] National Key Laboratory of Plant Physiology and Biochemistry of China, Beijing

Received December 13, 2002; accepted March 11, 2003; published online December 19, 2003

Summary. Pollen and skeletal muscle actins were purified and labeled with fluorescent dyes that have different emission wavelengths. Observation by electron microscopy shows that the fluorescent actins are capable to polymerize into filamentous actin in vitro, bind to myosin S-1 fragments, and have a critical concentration similar to unlabeled actin, indicating that they are functionally active. The globular actins from two sources were mixed and polymerized by the addition of ATP and salts. The copolymerization experiment shows that when excited by light of the appropriate wavelength, both red actin filaments (pollen actin) and green actin filaments (muscle actin) can be visualized under the microscope, but no filaments exhibiting both green and red colors are detected. Furthermore, coprecipitations of labeled pollen actin with unlabeled pollen and skeletal muscle actin were performed. Measurements of fluorescent intensity show that the amount of labeled pollen actin precipitating with pollen actin was much higher than that with skeletal muscle actin, indicating that pollen and muscle actin tend not to form heteropolymers. Injection of labeled pollen actin into living stamen hair cells results in the formation of normal actin filaments in transvacuolar strands and the cortical cytoplasm. In contrast, labeled skeletal muscle actin has detrimental effects on the cellular architecture. The results from coinjection of the actin-disrupting reagent cytochalasin D with pollen actin show that overexpression of pollen actin prolongs the displacement of the nucleus and facilitates the recovery of the nuclear position, actin filament architecture, and transvacuolar strands. However, muscle actin perturbs actin filaments when injected into stamen hair cells. Moreover, nuclear displacement occurs more rapidly when cytochalasin D and muscle actin are coinjected into the cell. It is concluded that actins from plant and animal sources behave differently in vitro and in vivo and that they are functionally not interchangeable.

Keywords: Actin; Actin derivatization; Polymerization; Microinjection; *Tradescantia virginiana*; Stamen hair cell.

* Correspondence and reprints: Institute of Cell Biology, College of Life Science, Beijing Normal University, Beijing 100875, People's Republic of China.
E-mail: hren@bnu.edu.cn

Introduction

Actin is one of the most ubiquitous, abundant proteins in eukaryotic cells and participates in many important subcellular processes. Actin genes have been highly conserved during evolution and the protein sequences among different eukaryotic actins share 83–88% amino acid identity (McDowell et al. 1996). Despite the high sequence identity and similarities in charge, molecular weight, and some biophysical and biochemical properties (Kim et al. 1996, Yen et al. 1995, Ren et al. 1997), actins from different sources have also shown some functional differences (Kim et al. 1996). Yeast (*Saccharomyces cerevisiae*) actin characteristics differ from those of skeletal muscle actin (Buzan et al. 1996, Kim et al. 1996), e.g., yeast actin polymerizes at a faster rate than muscle actin and produces less force when interacting with heavy meromyosin. Plant pollen actin was found to have a shorter lag period for assembly and faster rate of polymerization than rabbit skeletal muscle actin, and the value of the critical concentration of plant pollen actin polymerization is higher than that of rabbit skeletal muscle actin (Ren et al. 1997). As it is well known, most plant and animal genes are members of gene families that are differentially expressed and may encode diverse protein isovariants. Actin genes show distinct but overlapping expression patterns. Hence, cells may contain different actin isoforms. A number of observations suggest that distinct actin isoforms are functionally specialized (Ohmori et al. 1992, Hill and Gunning 1993, Fyrberg et al. 1998). From various experimental results, it is considered that highly variable plant actin isovariants may vary in their physical chemical parameters and may interact differentially with some actin-binding proteins

(reviewed in Meagher et al. 1999). It would be of interest to know whether those actin isoforms polymerize into homopolymers separately or copolymerize into heteropolymers, and whether they function differently in cells.

Mammalian tubulins have been successfully employed to study the microtubule behavior in plant cells. They incorporate with plant microtubule arrays and function normally after labeling with fluorescent dyes and injection into plant cells (Zhang et al. 1990, Hepler et al. 1993, Yuan et al. 1994). Surprisingly, the introduction of animal actins into plant cells has so far not succeeded. The introduction of purified rabbit skeletal muscle actin into plant cells had different effects on cellular architecture and actin organization (Ren et al. 1997).

In the present study, fluorescent actin analogues and microinjection of actins from plant and animal sources were used to test further the polymerization behavior of different actins in vitro and in living plant cells. Our goal is to investigate whether these actins could form heteropolymers and whether animal actins could incorporate with the plant actin cytoskeleton and function in vivo.

Material and methods

Reagents

Oregon Green 488 carboxylic acid succinimidyl ester, 5-(and-6)-carboxytetramethylrhodamine succinimidyl ester, and Alexa 488-phalloidin were purchased from Molecular Probes (Eugene, Oreg., U.S.A.). Cytochalasin D (CD) and dithiothreitol were from Sigma (St. Louis, Mo., U.S.A.). ATP was from Boehringer Mannheim (Roche Diagnostics, Indianapolis, Ind., U.S.A.). SM-2 adsorbent was from Bio-Rad (Hercules, Calif., U.S.A.). Injection buffer: 2 mM Tris-acetate, 0.1 mM dithiothreitol, 0.2 mM ATP, 5 mM $MgCl_2$, pH 7.5. Buffer M: 5 mM Tris-acetate, 0.2 mM dithiothreitol, pH 7.5. G-buffer: 5 mM Tris-HCl, pH 8.0, 0.2 mM $CaCl_2$, 0.2 mM ATP, 0.5 mM dithiothreitol, 0.01% NaN_3.

Purification and derivatization of pollen and muscle actin

Pollen actin was prepared from maize (*Zea mays*) pollen by the method of Ren et al. (1997). Skeletal muscle actin was purified from New Zealand white rabbits by the method of Pardee and Spudich (1982). Purified actin from both sources was stored in G-buffer at −80 °C.

Purified pollen actin was derivatized with carboxytetramethylrhodamine succinimidyl ester or Oregon Green 488 carboxylic acid succinimidyl ester and muscle actin was derivatized with Oregon Green 488 carboxylic acid succinimidyl ester by the method of Ren (1999). After removing the free dye with SM-2 beads, labeled actin was subjected to one polymerization-depolymerization cycle and dialyzed against actin injection buffer, then divided into 5 μl aliquots and stored at −80 °C for microinjection experiments, or dialyzed against G-buffer, divided into 5 μl aliquots, and stored at −80 °C.

Sodium dodecyl sulfate-polyacrylamide gel electrophoresis and determination of protein concentration

Fluorescent actin analogues were electrophoresed on a 15% sodium dodecyl sulfate-polyacrylamide gel and stained with Coomassie blue. A Bio-Rad Protein Assay Kit II was used for protein concentration determination using bovine serum albumin as standard.

Decoration of derivatized actin filaments with myosin S-1 fragment and negative staining

Myosin S-1 fragment was prepared from the skeletal muscle myosin that was purified from the back muscle of a New Zealand white rabbit by the method of Weeds et al. (1975). For actin filament decoration, 10 μl of 10 μM derivatized actin was polymerized by the addition of $MgCl_2$ and KCl to final concentrations of 5 mM and 100 mM, respectively, and incubated for 2 h. To the solution of polymerized actin filaments 5 μl of a solution of S-1 fragment at a concentration of 0.8 mg/ml was then added and stirred carefully for mixing. The mixture was kept on ice for 1 h before observation. For the visualization of the actin structure, samples were applied to Formvar-plus-carbon-coated grids and negatively stained with 2% uranyl acetate. The specimen was visualized in a transmission electron microscope (Hitachi-H 600; Hitachi, Tokyo, Japan). Negative staining of derivatized actin filaments without S-1 fragment was also performed as a control.

Determination of critical concentration for derivatized-actin polymerization

For the determination of critical concentrations, 500 μl samples containing 0.25, 0.5, 1.0, 1.5, 2.0, 2.5, 3.0 μM of derivatized globular actin (G-actin) from pollen in G-buffer were prepared. At time zero, ATP, $MgCl_2$, and KCl were added to final concentrations of 2 mM, 5 mM, and 100 mM, respectively, and incubated for 16 h. Steady-state polymer levels were measured by 90 °C light scattering with a fluorescence spectrophotometer (FluoroMax-II; Instrument SA, Edison, N.J., U.S.A.) set for excitation and emission wavelengths of 450 nm. Readings from same concentration of derivatized G-actin were used as controls.

Copolymerization of pollen and muscle actin in vitro

20 μl of 4 μM derivatized pollen actin (labeled with carboxytetramethylrhodamine) and rabbit skeletal muscle actin (labeled with Oregon Green 488) were mixed in an Eppendorf tube. Polymerized actin was achieved by addition of ATP, $MgCl_2$, and KCl to final concentrations of 2 mM, 5 mM, and 100 mM, respectively, and incubated for 10 h. The actin filaments were observed on a confocal laser scanning microscope (MRC 1024; Bio-Rad) using illumination with the 567 nm line of the Kr-Ar laser for red-fluorescent filaments (pollen actin) or the 488 nm line for green-fluorescent filaments (muscle actin). The same experiment was repeated with pollen actins labeled with carboxytetramethylrhodamine and with Oregon Green 488.

For coprecipitation measurements, fluorescent pollen G-actin was added into 500 μl of 3 μM pollen actin or rabbit skeletal muscle actin to a final concentration of 0.3 μM (which is below the critical concentration) or 0.6 μM (above the critical concentration), respectively. Then the samples were added to 2 mM ATP, 5 mM $MgCl_2$, and 100 mM KCl and incubated for 16 h. Polymerized actins were precipitated by centrifugation at 100,000 **g** for 1 h. The pellet was resuspended with 500 μl of methanol, and then the emission fluorescence value was measured with a fluorescence spectrophotometer using an illumination of 496 nm wavelength. The polymerization buffer with only 0.3 μM fluorescent pollen actin (which is below the critical concentration) served as control.

Microinjection of stamen hair cells

Stamen hairs were collected from open flowers of *Tradescantia virginiana* and immobilized for microinjection (Staiger et al. 1994, Ren et al. 1997). Only cells with a nucleus positioned in the middle of the cell and supported

by transvacuolar strands were injected. Needles were tip-filled to a measured distance from needle tip that was equivalent to a volume of 5 pl or 10 pl (for comicroinjection) estimated by the injection of the same volume of oil. Assuming that the vacuole occupies between 80 and 90% of the total cell volume, the injectate was approximately 10% or 20% of the cytoplasmic volume. The needle concentration of CD was 20 μM and that of actin was 34 μM. The in vivo effects of CD and G-actin of different sources were compared by monitoring their disruptive and reconstructive effect on the actin-dependent position of the nucleus (Gibbon et al. 1997, Ren et al. 1997). Time zero was marked when the entire contents of the injection entered the cytoplasm, and each cell was monitored for a maximum of 60 min. Displacement and resumption of the position of the nucleus was monitored by measuring the time for the nucleus to move completely outside the perimeter and move back, defined by its edge at time zero.

The concentration of purified actin or fluorescently labeled actin for microinjection was 34 μM. In some cases, filamentous actin (F-actin) in living stamen hair cells was stained by double-injection of Alexa 488-phalloidin. Images were acquired with a confocal laser scanning microscope (MRC 1024; Bio-Rad). Alexa 488-phalloidin was dissolved in methanol to a concentration of 6.6 μM and stored frozen in small aliquots. For injection, a fresh aliquot was air dried and resuspended in microinjection buffer (buffer M) to a final concentration of 8 μM.

The needle, which remained in the cell for 5–8 min, was removed from the cell after microinjection. A coverslip was applied prior to observations. Cells were imaged through a ×40 plan apo objective (numerical aperture, 1.0) at the illumination of the 488 nm line of the Kr-Ar laser. Optical sections in 0.8–1 μm steps were collected and projected with an imaging software package. Images were further processed with Adobe Photoshop 6.0.

Results

In vitro polymerization of fluorescent actin analogues

Maize pollen actin was labeled with carboxytetramethylrhodamine or Oregon Green 488, and muscle actin was derivatized with Oregon Green 488. A yield of 3 mg of fluorescent actin analogue was obtained from 10 mg of maize pollen actin with a dye-to-protein ratio of 72% and 4 mg of fluorescent actin analogue was obtained from 10 mg of rabbit skeletal muscle actin with a dye-to-protein ratio of 70%. Densitometric analysis of the gel from sodium dodecyl sulfate-polyacrylamide gel electrophoresis of fluorescent actin analogues indicates that the purity of actin analogues was as high as 98% (Fig. 1). The fluorescent actin analogues polymerized in vitro into filaments by the addition of Mg^{2+} and K^{+}. Further, assembly and disassembly of the fluorescent actin analogues showed that their polymerization activity was repeatable. The quality of derivatized actin and the ability of its binding to the myosin S-1 fragment were further analyzed by negative staining of in vitro polymerized F-actin. Figure 2 shows an example of derivatized pollen actin filaments and decoration with myosin S-1 fragments. Figure 2 A shows that the derivatized actin could form long straight or curved polymers with an average diameter of around 6 nm; the filaments decorated with myosin S-1 are

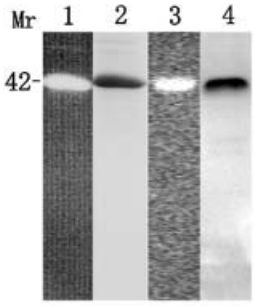

Fig. 1. Derivatized plant actin analogue in sodium dodecyl sulfate-polyacrylamide gel stimulated by ultraviolet radiation (*1*) and stained with Coomassie blue (*2*); derivatized rabbit skeletal muscle actin analogue in sodium dodecyl sulfate-polyacrylamide gel stimulated by ultraviolet radiation (*3*) and stained with Coomassie blue (*4*)

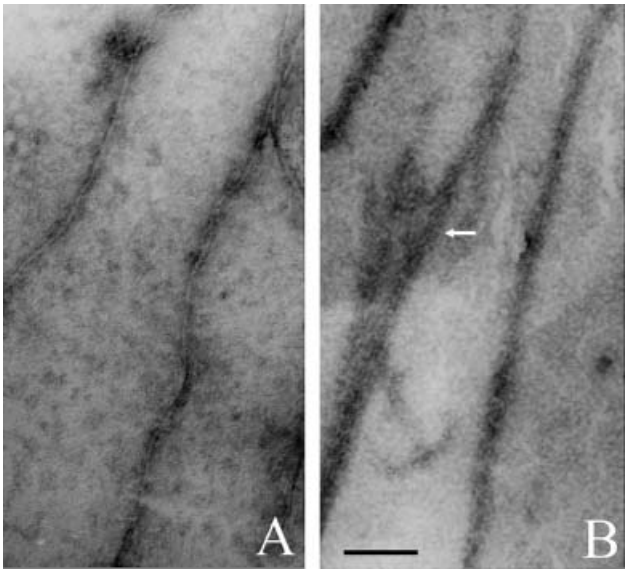

Fig. 2 A, B. Actin filaments polymerized from derivatized actin analogues and decoration by myosin S-1 fragment. **A** Long straight or curved actin filaments polymerized from derivatized pollen actin analogues visualized by negative staining and electron microscopy. **B** Derivatized pollen actin filaments decorated with myosin S-1 fragment by negative staining and electron microscopy. Bar: 100 nm

about 25 nm in diameter. At higher magnification, some regions of the decorated filaments appear as characteristic arrowhead structures (Fig. 2 B). Light-scattering measurement shows that the average value of the critical concentration for derivatized pollen actin from three experiments was 0.45 ± 0.07 μM (Fig. 3), which was similar to that of unlabeled pollen actin (Ren et al. 1997).

Pollen actin and rabbit skeletal muscle actin tend not to form heteropolymers

We successfully labeled animal and plant actins with Oregon Green 488 and carboxytetramethylrhodamine fluorescent probes, respectively. Animal and plant actins

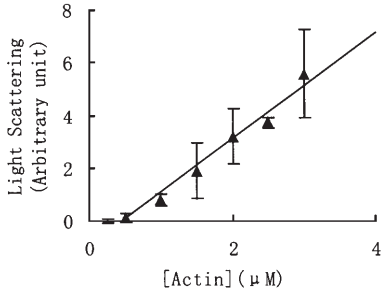

Fig. 3. Determination of critical concentration for derivatized pollen actin polymerization. Samples containing 0.25, 0.5, 1, 1.5, 2, 2.5, and 3 μM derivatized pollen G-actin in G-buffer were polymerized for 16 h by the addition of ATP, $MgCl_2$, and KCl as given in the Material and methods section. The amount of polymer at each actin concentration was measured by light scattering at steady state, normalized against identical samples without salt, and plotted versus the total actin concentration. The intercept with the x-axis of a line of best fit through these data defines the critical concentration. The mean critical concentration (with standard deviation) of derivatized pollen actin was 0.45 ± 0.07 μM (n = 3)

share many similarities in physical and chemical properties. However, there exist some differences between plant and animal actins in their biochemical properties and some distinct functions in vitro and in vivo (Ren et al. 1997, Kovar et al. 2001). We used two fluorescent actin analogues to investigate whether they could copolymerize to form heteropolymers in vitro.

In specimens in which just one kind of fluorescent actin analogue was used to polymerize, fluorescent filaments could be clearly imaged only when the specimens were illuminated with the appropriate excitation wavelength. Pollen actin filaments exhibited red-fluorescent images when excited by light with a wavelength of 567 nm (Fig. 4A), whereas no filaments could be detected at an excitation wavelength of 488 nm. However, actin filaments polymerized from fluorescent skeletal muscle actin exhibited green-fluorescent images when excited by light with a wavelength of 488 nm (Fig. 4B), and there was no obvious image at an excitation wavelength 567 nm. When mixtures of pollen and skeletal muscle actin analogues were excited by light with a wavelength of 567 nm and/or 488 nm, there were red actin filaments appearing in some areas (Fig. 4C), but no green actin filaments were detected in the same areas (Fig. 4D). On the other hand, there were green actin filaments appearing in some other areas (Fig. 4E), whereas no red actin filaments appeared in these regions (Fig. 4F). No filaments exhibiting both green and red color were detected. Nevertheless, in some areas, both red filaments (Fig. 4G) and green filaments (Fig. 4H) could be found, but they did not overlap (Fig. 4I). Interestingly, muscle skeletal actin could not form straight filaments but formed curved actin bundles in the mixtures (Fig. 4E, H). However, when two pollen actins with different fluorescence were copolymerized, both red-fluorescent filaments (excited by light with a wavelength of 567 nm) and green-fluorescent filaments (excited by light with a wavelength of 488 nm) could be visualized in all areas (Fig. 4J, K). Furthermore, those red filaments and green filaments were overlapping (Fig. 4L).

Considering the sensitivity limit of the microscopy for the detection of trace heteropolymers, the more sensitive fluorescence intensity measurement was used for further examination in coprecipitation experiments. Fluorescent pollen G-actin with a final concentration of 0.3 μM or 0.6 μM was added to 3 μM pollen actin or rabbit skeletal muscle actin. The polymerized actin was precipitated and measured with a fluorescence spectrophotometer. The results showed that for concentrations below as well as above the critical concentration (0.45 μM), the amount of labeled pollen actin precipitating with pollen actin was much higher than that precipitating with skeletal muscle actin, about 5 times higher at the subcritical concentration and 7 times higher at the supercritical concentration (Fig. 5). This result indicates that fluorescent pollen actin copolymerizes with pollen actin much easier than with rabbit skeletal muscle actin.

All in all, it can be concluded that actin monomers from animal and plant cell tend to form homopolymers but not heteropolymers in vitro.

Pollen and rabbit skeletal muscle actins do not behave similarly in living plant cells

To examine the effects of the introduction of pollen actin and skeletal muscle actin into living plant cells, we injected Oregon Green 488-labeled pollen actin and skeletal muscle actin into *T. virginiana* stamen hair cells. Using the microinjection method, about 10 pl of fluorescent actin analogues with a concentration of 34 μM was introduced into the cytosol of stamen hair cells. The injection of fluorescently labeled skeletal muscle actin had remarkable effects on the cellular architecture, disrupted the cytoplasmic streaming, and accumulated in cellular organelles. At the same time, a massive array of green-fluorescent filaments appeared at the site of injection (Fig. 6A). In contrast, the injection of fluorescently labeled pollen actin led to the formation of normal actin filaments in transvacuolar strands and the cortical cytoplasm (Fig. 6B).

To test further the functional differences between pollen actin and skeletal muscle actin, we conducted three kinds of microinjection into *T. virginiana* stamen

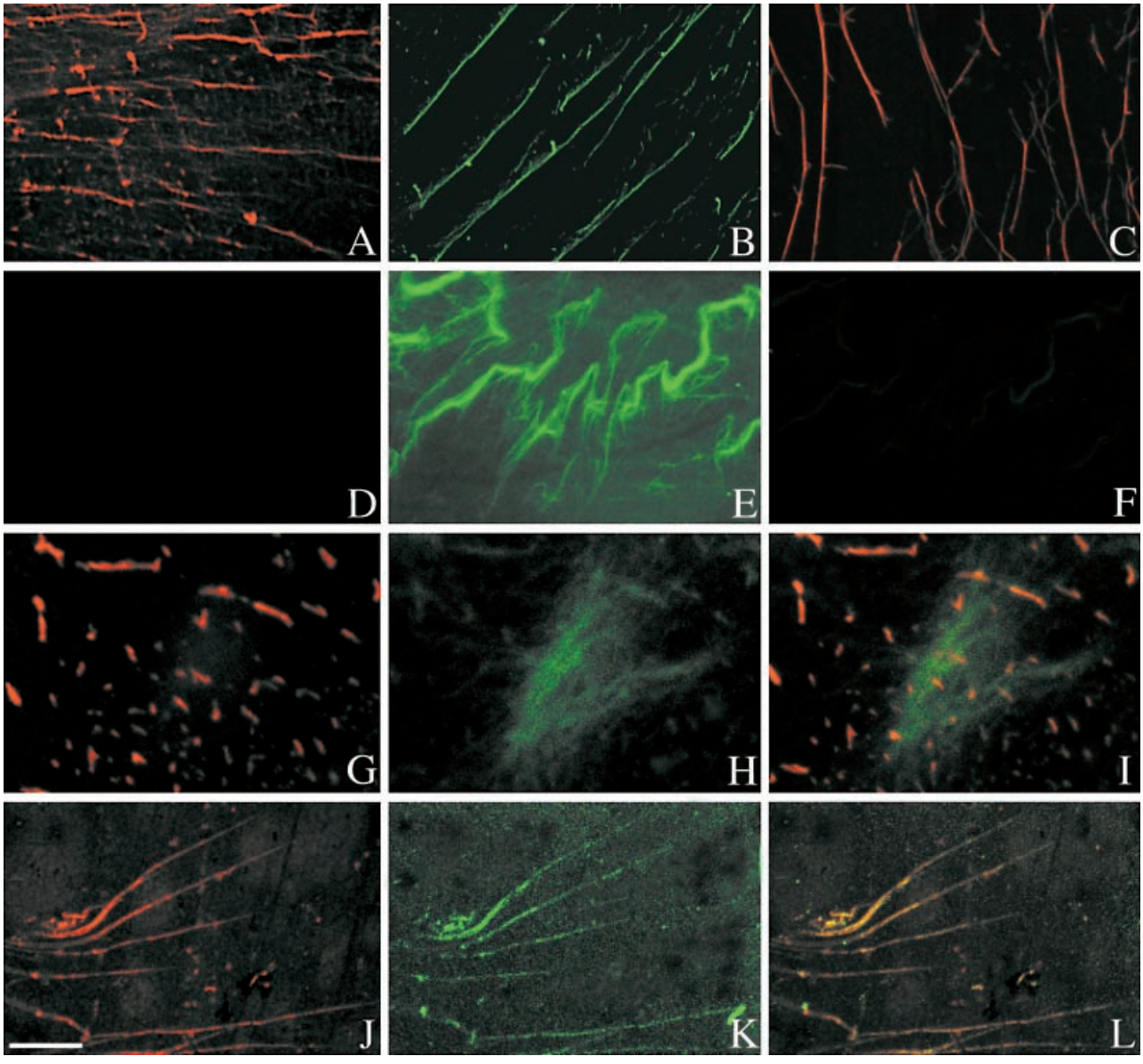

Fig. 4 A–L. Copolymerization of actins from pollen and skeletal muscle actin analogues. **A** Filaments composed from pollen actin fluorescent analogue appear as red fluorescent filaments when excited by light with a wavelength of 567 nm. **B** Filaments composed from skeletal muscle actin fluorescent analogue appear as green fluorescent filaments when excited by light with a wavelength of 488 nm. **C** and **D** When pollen and skeletal muscle actin analogues are copolymerized, red-fluorescent filaments can be visualized in some areas when excited by light with a wavelength of 567 nm (**C**), whereas no green-fluorescent filaments are present at an excitation wavelength of 488 nm (**D**). **E** and **F** In some other areas, green-fluorescent filaments are present when excited by light with a wavelength of 488 nm (**E**), but no red actin filaments appeared at an excitation wavelength of 567 nm (**F**). **G–I** There are however some areas where both red-fluorescent filaments (**G**) and green-fluorescent filaments (**H**) can be found, but they are not overlapping (**I**). **J–L** When two fluorescent pollen actin analogues copolymerized, red-fluorescent filaments can be visualized when excited by light with a wavelength of 567 nm (**J**) and green-fluorescent filaments are also present when excited by light with a wavelength of 488 nm in all areas (**K**), and the filaments are overlapping (**L**). Bar: 10 μm

hair cells: CD alone, coinjection of CD with pollen actin, coinjection of CD with muscle actin (actins used here were unlabeled). All microinjections caused transvacuolar strands to become thinner and snap, cytoplasmic streaming ceased, and the nucleus was displaced from the center position of the cell. However, the length of time for the nucleus to move one nuclear diameter from its original position after the microinjection and subsequently to move back, taken as an indication of the recovery, was quite different among the three kinds of microinjections. As shown in Table 1, the average time for nuclear displacement after microinjection of CD and pollen actin (13.4 min) was a little longer than that of CD alone (11.2 min). On the other

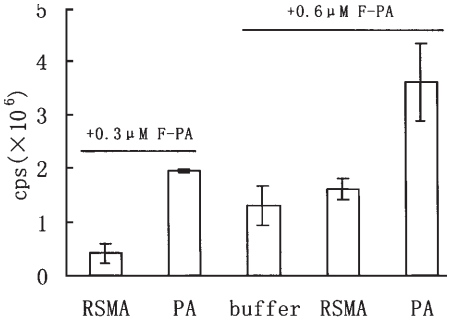

Fig. 5. Coprecipitation of actins from pollen and skeletal muscle actin. Samples containing 3 μM rabbit skeletal muscle actin (*RSMA*) or 3 μM maize pollen actin (*PA*) were copolymerized with 0.3 μM (subcritical concentration) or 0.6 μM fluorescent pollen G-actin (*F-PA*) (supercritical concentration). To assay the amount of fluorescent pollen actin's self-polymerization above the critical concentration, a sample containing 0.6 μM fluorescent pollen actin in G-buffer was also included. The polymerized actins were precipitated and the emission fluorescence values were measured. The values were plotted as the means (with standard deviations) of three experiments after normalization of the interference of fluorescence in the polymerization buffer containing 0.3 μM fluorescent pollen actin. From the comparison of the portions of fluorescent pollen actin incorporated into maize pollen actin and rabbit skeletal muscle actin, it was calculated that about 5 times and 7 times more fluorescent pollen actin incorporated with maize pollen actin than with rabbit skeletal muscle actin below and above the critical concentration, respectively

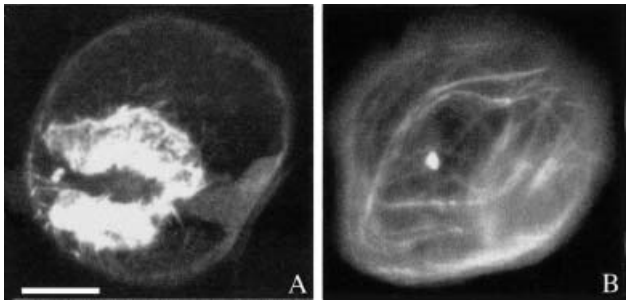

Fig. 6. **A** *Tradescantia virginiana* stamen hair cell injected with fluorescent skeletal muscle actin shows aberrant microfilament arrays. **B** *Tradescantia virginiana* stamen hair cell injected with fluorescent pollen actin shows normal actin filaments. Bar: 20 μm

hand, the average time for nuclear displacement after microinjection of CD and muscle actin (5.4 min) was much shorter than that of CD alone. The average time for nuclear displacement with CD and pollen actin coinjection was significantly different from that of the injection of CD ($P \leqslant 0.005$) or CD plus muscle actin ($P \leqslant 0.001$). Moreover, nuclear repositioning and cytoplasmic streaming in cells coinjected with CD and pollen actin could recover within 50 min, whereas those injected with CD alone or CD with muscle actin could not recover during the time periods of our observation (about 60 min). Injection of buffer alone or pollen actin alone had little effect on nuclear displacement. These results demonstrate that pollen actin may facilitate the

Table 1. Duration of displacement of nucleus[a]

Injectate	Mean time of nuclear displacement (min)	Mean time of recovery of central position (min)
CD	11.2 ± 1.5	no recovery[b]
CD + pollen actin	13.4 ± 5.1	50.1 ± 5.7
CD + muscle actin	5.4 ± 2.3	no recovery[b]
Injection buffer	>20.0	nd[c]
Pollen actin	>20.0	nd

[a] The average time required for nuclei to move one nuclear diameter from the original position and their return to the original position was measured after *T. virginiana* stamen hair cells were injected with 20 μM CD or 20 μM CD plus 34 μM actin. Injected cells were monitored for a maximum period of 60 min. Values are means with standard deviations for n = 13 each

[b] No recovery was detected within the maximum observation period

[c] Not done

recovery of the actin filament architecture in living plant cells, whereas muscle actin perturbs actin filaments in living plant cells.

Furthermore, a series of double microinjections was performed to determine the organization of the actin cytoskeleton in living stamen hair cells. Alexa 488-phalloidin was microinjected into the cells 20 or 60 min after the introduction of CD alone, CD plus pollen actin, or CD plus muscle actin. The injection of CD alone, CD plus pollen actin, or CD plus muscle actin all caused the endogenous F-actin network to be destroyed, transvacuolar strands and cortical actin filaments disappeared. Only some random short fragments could be seen (Fig. 7A–C). In most cells injected with CD alone, there were no obvious changes of this situation within 60 min after the injection. In a few cells, though, fine cortical actin filaments appeared (Fig. 7D), but transvacuolar strands (Fig. 7G) and recovery of the central nuclear position (not shown) did not occur. In cells that were coinjected with CD and skeletal muscle actin, the actin filaments in cortical or transvacuolar strands never reappeared during our observations (Fig. 7F, I). In cells that were coinjected with CD and pollen actin, cortical actin filaments and transvacuolar strands could be seen again after the nuclei recovered their position and cytoplasmic streaming recommenced (Fig. 7E, H).

Discussion

Pollen and muscle skeletal actin isoforms tend not to form heteropolymers in vitro and in vivo

Fluorescent-analogue cytochemistry has been used extensively to study the dynamic nature of the cytoskeletal orga-

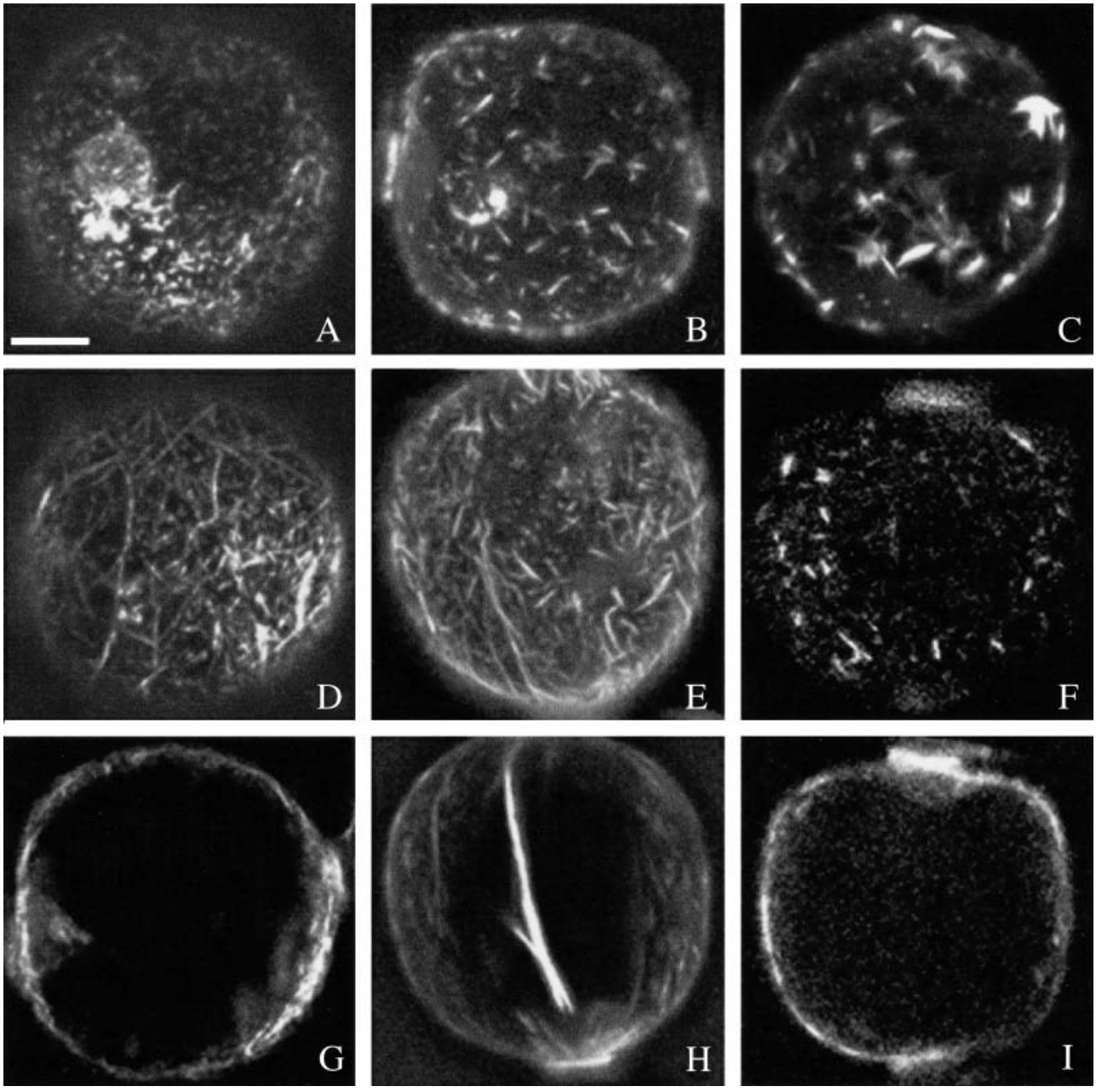

Fig. 7 A–I. Reorganization of the actin cytoskeleton in *T. virginiana* stamen hair cells after microinjection. **A–C** 20 min after injection, cells injected with CD alone (**A**), CD plus pollen actin (**B**), and CD plus muscle actin (**C**) all exhibited a pattern of randomly arranged short actin fragments, stained by injection of Alexa 488-phalloidin. **D–I** 60 min after injection, fine cortical actin cytoskeleton reappears in cells injected with CD alone (**D**) and CD plus pollen actin (**E**), while no actin filaments can be detected in the cell injected with CD plus skeletal muscle actin (**F**). In addition, a few transvacuolar actin strands could be seen in the cell injected with CD plus pollen actin (**H**), although no transvacuolar actin filaments could be seen in cells injected with CD alone (**G**) or CD plus skeletal muscle actin (**I**). Bar: 20 μm

nization in living cells (Wang et al. 1980, Giuliano et al. 1985). But the application of this method on studies of actin cytoskeleton in plant cells is still exceptional (Ren et al. 2000; Kovar et al. 2001a, b). We reported previously two methods for labeling plant actin with fluorescent dye at free amino groups and thiol groups (Ren et al. 1999, 2000). Our results showed that both the yield of fluorescent analogue and its dye-to-protein ratio were as high as that with the method reported for animal cell studies (Wang et al. 1980). In the present study, the method for labeling actin at free amino groups was used to label the actin from maize pollen and rabbit skeletal muscle actin with different fluorescent dyes. With electron microscopy and confocal laser scanning microscopy, it was shown that

they both could not only polymerize in vitro but also be decorated by myosin S-1 fragments to form arrowhead structures and have a similar critical concentration with unlabeled actin. The results demonstrated that the fluorescent actin analogues obtained by our methods are as active as their original actins in their polymerization property.

Our preliminary results showed that the introduction of purified pollen actin or rabbit skeletal muscle actin into plant cells had different effects on the cellular architecture and actin organization (Ren et al. 1997). However, there are still no direct experimental evidences to show whether different actin isoforms can form a heteropolymer or not. In this study, fluorescent actin analogues combined with different examination methods have been used to detect the behavior of actins from plant and animal sources incubated in vitro in the same solution. Although the heteropolymer cannot be visualized by fluorescent microscopy, it is shown by fluorescence spectrophotometry that there are indeed only very small amounts of labeled pollen actin precipitating with rabbit skeletal muscle actin even when the labeled pollen actin is below the critical concentration. However, the amount of labeled pollen actin precipitating with pollen actin is much higher. From the above results, it is indicated at least that actin from animal and pollen sources does not tend to form heteropolymers. Although the actins used in the present experiments are a mixture of different isoforms from pollen sources, there is one major isoform in maize pollen (Ren et al. 1997).

In our in vivo experiments, pollen actin or skeletal muscle actin was introduced into *T. virginiana* stamen hair cells. The injection of fluorescently labeled pollen actin resulted in the formation of normal actin filaments in transvacuolar strands and the cortical cytoplasm. In contrast, the injection of fluorescent skeletal muscle actin had significant effects on the cellular architecture and a massive array of actin filaments was formed at the injection site. This behavior is similar to that observed previously with unlabled actin (Ren et al. 1997). The actin-disrupting reagent CD was injected with pollen actin or muscle actin, and nuclear displacement as well as subsequent recovery of transvacuolar strands and reorganization of the actin cytoskeleton were observed. The results showed that pollen actin facilitates the recovery of the nuclear position and the actin filament architecture, suggesting that pollen actin enters the actin cytoskeleton by actin turnover and functions in living plant cells. However, muscle actin formed a massive array at the injection site and perturbed actin filaments in living plant cells. Moreover, the nuclear displacement occurred more rapidly when CD and muscle actin were coinjected into the cell and no recovery was seen within 60 min after the injection. When CD and pollen actin were coinjected, the nuclear displacement was prolonged. The actin cytoskeleton and transvacuolar strands were recovered, and the nucleus moved back to its central position in the cell after about 50 min. From the above results it is concluded that actin from plant and animal sources are not tending to form heteropolymers and they are not functionally interchangeable.

Actin isoforms may form different actin filaments to play different roles in cells

Actin proteins are encoded by multiple gene families that are expressed in the organism temporally and spatially in distinct patterns. Higher-plant actin genes encode proteins that are relatively divergent in their primary structures compared with actin proteins from other kingdoms (Meagher et al. 1999). This protein diversity may be due to functional differences. A number of observations in animal cells strongly support that different actin isoforms have unique properties and are not functionally equivalent (Rubenstein 1990, Herman 1993, Fyrberg et al. 1998). The functional significance of the actin isovariants in plants, however, has not yet been studied in detail.

Meagher et al. (1999) presented a hypothesis for isovariant dynamics, suggesting that the simultaneous expression and interaction of multiple isovariants of actin may expand cytoskeletal responses to signal transduction and functions in developmental processes. Potentially, different actin isoforms may polymerize into homopolymers or heteropolymers. Meagher et al. (1999) suggested that the degree of heteropolymer formation depends on monomer concentrations and the specific K_d values for association between actin isoforms. Our experiments show that actin from animal and pollen sources do not tend to form heteropolymers but tend to form homopolymers even at the same monomer concentrations. When injected into living plant cells, pollen actins can incorporate with the actin cytoskeleton in the cell, while it seems that most muscle skeletal actins are organized separately from the actin cytoskeleton of the cell. Our observations suggest that actin isoforms may form different actin filaments which may serve for various functions in the cell. Similar experiments will need to be performed with fluorescently tagged plant actin isovariants.

Using site-directed mutagenesis, Fyrberg et al. (1998) tested the amino acid replacements of six genes of *Drosophila melanogaster* that encode conventional actins and found that these actin isoforms are not interchangeable and that actin isoform sequences are not equivalent. For maize

pollen treated with low concentrations of the actin inhibitor Latrunculin B, Gibbon et al. (1999) revealed that pollen tube growth is much more sensitive to F-actin disruption than pollen germination. They proposed that there exists a small population of Latrunculin B-sensitive actin filaments which is critical for the maintenance of tip growth but not for pollen germination. Although the mechanism which makes the difference of F-actin populations is still not clear, one possibility to be considered is that those different actin filaments are made up of different actin isoforms or different ratios of actin isoforms. Our experimental results strongly support that different populations of actin filaments tend to be made up of different actin isoforms.

Acknowledgments

We thank Chris Staiger (Purdue University) and Ming Yuan (China Agricultural University) for critical reading and comments on the manuscript. This work was supported by grants of the Major State Basic Research Development Program of the People's Republic of China (G19990117) and the National Natural Science Foundation of China (39870052). Y. Jing and K. Yi are considered joint first authors.

Reference

Buzan JM, Frieden C (1996) Yeast actin: polymerization kinetic studies of wild type and a poorly polymerizing mutant. Proc Natl Acad Sci USA 93: 91–95

Fyrberg EA, Fyrberg CC, Briggs JR, Saville D, Beall CJ, Detchum A (1998) Functional non-equivalence of *Drosophila* actin isoforms. Biochem Genet 36: 271–287

Gibbon BC, Ren HY, Staiger CJ (1997) Characterization of maize (*Zea mays*) pollen function in vitro and in live cells. Biochem J 327: 909–915

– Kovar DR, Staiger CJ (1999) Latrunculin B has different effects on pollen germination and tube growth. Plant Cell 11: 2349–2363

Giuliano KA, Taylor DL (1995) Measurement and manipulation of cytoskeletal dynamics in living cells. Curr Opin Cell Biol 7: 4–12

Hepler PK, Cleary AR, Gunning BES, Wadsworth P, Wasteneys GO, Zhang DH (1993) Cytoskeletal dynamics in living plant cells. Cell Biol Int Rep 17: 127–142

Herman IM (1993) Actin isoforms. Curr Opin Cell Biol 5: 48–55

Hill MA, Gunning P (1993) Beta and gamma actin mRNAs are differentially located within myoblasts. J Cell Biol 122: 825–832

Kim E, Miller CJ, Reisler E (1996) Polymerization and in vitro motility properties of yeast actin: a comparison with rabbit skeletal α-actin. Biochemistry 35: 16566–16572

Kovar DR, Gibbon BC, McCurdy DW, Staiger CJ (2001a) Fluorescently labeled fimbrin decorates a dynamic actin filament network in live plant cells. Planta 213: 390–395

– Yang P, Sale WS, Drobak BK, Staiger CJ (2001b) *Chlamydomonas reinhardtii* produces a profilin with unusual biochemical properties. J. Cell Sci 114: 4293–4305

McDowell JM, Huang SR, McKinney EC, An YQ, Meagher RB (1996) Structure and evolution of the actin gene family in *Arabidopsis thaliana*. Genetics 142: 587–602

Meagher RB, McKinney EC, Kandasamy MK (1999) Isovariant dynamics expands and buffers the responses of complex systems: the diverse plant actin gene family. Plant Cell 11: 1–12

Ohmori H, Toyama S, Toyama S (1992) Direct proof that the primary site of action of cytochalasin on cell motility processes is actin. J Cell Biol 116: 933–941

Pardee JD, Spudich JA (1982) Purification of muscle actin. Methods Cell Biol 24: 271–289

Ren HY (1999) Preparation of actin and fluorescent actin analogs from plant cell. Acta Bot Sin 41: 1099–1103

– Yuan M (2000) Polymerization of fluorescent analogue of plant actin in vitro and in vivo. Chin Sci Bull 45: 1583–1586

– Gibbon BC, Ashworth SL, Sherman DM, Yuan M, Staiger CJ (1997) Actin purified from maize pollen functions in living plant cells. Plant Cell 9: 1445–1457

Rubenstein PA (1990) The functional importance of multiple actin isoforms. Bioessays 12: 309–315

Staiger CJ, Yuan M, Valenta R, Shaw PJ, Warn RM, Lloyd CW (1994) Microinjection of profilin affects cytoplasmic streaming in plant cells by depolymerizing actin microfilaments. Curr Biol 4: 215–219

Wang YL, Taylor DL (1980) Preparation and characterization of a new molecular cytochemical probe: 5-iodoacetamidofluorescein-labeled actin. J Histochem Cytochem 11: 1198–1206

Weeds AG, Taylor RS (1975) Separation of subfragment-1 isoenzymes from rabbit skeletal muscle myosin. Nature 257: 54–56

Yen LF, Liu X, Cai ST (1995) Polymerization of actin from maize pollen. Plant Physiol 107: 73–76

Yuan M, Shaw PJ, Warn RM, Lloyd CW (1994) Dynamic reorientation of cortical microtubules, from transverse to longitudinal, in living plant cells. Proc Natl Acad Sci USA 91: 6050–6053

Zhang DH, Wadsworth P, Hepler PK (1990) Microtubule dynamics in living dividing plant cells: confocal image of microinjected fluorescent brain tubulin. Proc Natl Acad Sci USA 87: 8825–8829